Supplemental Figure Legends

Figure S1. Chemotherapy promotes $CD8^+$ T cell anti-tumor immunity (related to Figure 1)

A. Representative images of IHC staining of CD8 in the tumor tissues from breast cancer patients before neo-adjuvant chemotherapy (NCT) and after NCT. Scale bar: 100 μM.

B. Tumor growth curve of 4T1 in the WT mice treated with vehicle or chemotherapeutic drugs PTX as indicated. Data are shown as mean±SEM (n=4 mice per group). Two-way ANOVA (mixed model) and Sidak's multiple comparisons test were performed.

C. FACS analysis of tumor-infiltrating $CD3^+CD8^+$ T cells in the mice treated with vehicle or chemotherapy as **B** described. Data are shown as mean±SEM (n=5 mice per group). Two-way ANOVA and Sidak's multiple comparisons test were performed.

D. FACS analysis of DC ($CD45^+CD11c^+MHCII^{high}CD103^+$), macrophages ($CD45^+CD11b^+F4/80^+$), PMN-MDSC ($CD45^+CD11b^+Ly\text{-}6G^+Ly\text{-}6C^{low}$) and M-MDSC ($CD45^+CD11b^+Ly\text{-}6G^-Ly\text{-}6C^{low}$) in the tumor tissues of WT mice treated with vehicle or chemotherapeutic drugs PTX, DOX, CDDP as indicated. Data are shown as mean±SEM (n=5-6 mice per group). Two-way ANOVA (mixed model) and Sidak's multiple comparisons test were performed.

E. FACS analysis of $CD4^+$ and $CD8^+$ T cells in the splenocytes of WT mice treated

with anti-CD8 or IgG control antibodies upon chemotherapy treatment.

*, $P<0.05$; **, $P<0.01$; ***, $P<0.001$; ****, $P<0.0001$

Figure S2. Chemotherapy enhances tumor cell antigen presentation to facilitate $CD8^+$ T cell cytotoxic function (related to Figure 2)

A. Analysis of half maximal toxic concentration (IC_{50}) of chemotherapeutic drugs PTX, DOX, CDDP for E0771 cells.

B. Cell viability of E0771 exposed to chemotherapeutic drugs of PTX (20μM), DOX (3μM) and CDDP (20μM) by CCK8 assay. Quantitative data are shown as mean±SEM (n=3). Two-tailed unpaired t-test was performed for the comparisons between two groups.

C. Schematic illustration for the analysis of antigen-presenting ability of DC after co-cultured with the OVA expressing tumor cells (E0771-OVA or MC38-OVA) pretreated with vehicle or chemotherapeutic drugs PTX, DOX, CDDP for 24 hr.

D. FACS analysis of levels of MHC-I-complexed OVA peptide SIINFEKL on the surface of DC cells as **C** described.

E. Tumor growth curve of E0771-OVA-ZsGreen in the WT mice treated with vehicle or PTX. Data are shown as mean±SEM (n=5-6 mice per group). Two-way ANOVA (mixed model) and Sidak's multiple comparisons test were performed.

F. FACS analysis (left) and quantification (right) of levels of MHC-I-complexed OVA peptide SIINFEKL on the surface of DC($CD45^+CD11c^+MHCII^+CD103^+$) from draining lymph nodes in E0771-OVA-ZsGreen tumor-bearing mice with vehicle or PTX treatment. Quantitative data are shown as mean±SEM (n=5 mice per group).

Two-tailed unpaired t-test was performed for the comparisons between two groups.

G. Schematic illustration for functional analysis of naïve OT-1 $CD8^+$ T cells co-cultured with the OVA expressing tumor cells (E0771-OVA or MC38-OVA).

H. Representative FACS analysis of $IFN\gamma^+$ and Granzyme B^+ $CD8^+$ cells in OT-1 $CD8^+$ T cell as **G** described.

I. FACS analysis (left) and quantification (right) of $CD8^+$ T cells after OT-1 CTLs adoptive transfer in the E0771-OVA tumor-bearing *Rag2*$^{-/-}$ mice with vehicle or PTX treatment. Data are shown as mean±SEM (n=5-6 mice per group). Two-way ANOVA (mixed model) and Sidak's multiple comparisons test were performed.

J. FACS analysis (left) and quantification (right) of $IFN\gamma^+$ and Granzyme B^+ $CD8^+$ cells in the tumor tissue after OT-1 CTLs adoptive transfer in the E0771-OVA tumor-bearing *Rag2*$^{-/-}$ mice with vehicle or PTX treatment. Data are shown as mean±SEM (n=5 mice per group). Two-way ANOVA (mixed model) and Sidak's multiple comparisons test were performed.

*, $P<0.05$; **, $P<0.01$; ***, $P<0.001$; ****, $P<0.0001$; ns, non significance

Figure S3. Chemotherapy enhances $CD8^+$T cell activity through stimulating cancer cell-autonomous type I IFN production (related to Figure 3)

A. Representative of FACS for sorted tumor-infiltrating T cells ($CD45^+CD3^+$) and tumor cells ($CD45^-ZsGreen^+$) from E0771-OVA-ZsGreen tumor bearing mice after vehicle or PTX treatment.

B. GSEA analysis of enrichment of cell proliferation and apoptosis signatures in the tumor cells sorted from E0771-OVA-ZsGreen tumor bearing mice after vehicle or

PTX treatment.

C. Real-time PCR analysis of *Ifnb* and ISGs gene expression levels in 4T1 and MDA-MB-231 tumor cells after vehicle or indicated chemotherapeutic drugs treatment for 24 hr. Data are shown as mean±SEM (n=3). Two-way ANOVA and Sidak's multiple comparisons test were performed.

D. Percent lysis of MC38-OVA-Luc pretreated with the indicated chemotherapeutic drugs for 24 hr after incubation with OVA peptide activated OT-1 CTLs in the presence of anti-IFNAR1 neutralization antibody or IgG ctrl at the different ratios as shown. Data are shown as mean±SEM (n=3). Two-way ANOVA (mixed model) and Sidak's multiple comparisons test were performed.

E. FACS analysis of CD69 in tumor-infiltrating $CD8^+$T cells in E0771-OVA tumor-bearing WT and *Ifnar1*$^{-/-}$ mice with vehicle or PTX treatment. Data are shown as mean±SEM (n=4-5 mice). Two-way ANOVA and Sidak's multiple comparisons test were performed.

F. FACS analysis of IFNγ and Granzyme B staining in tumor-infiltrating $CD8^+$T cells in E0771-OVA tumor-bearing WT and *Ifnar1*$^{-/-}$ mice with vehicle or PTX treatment.

*, $P<0.05$; **, $P<0.01$; ***, $P<0.001$; ****, $P<0.0001$; ns, non significance

Figure S4. Cytosolic mtDNA in the tumor cells is required for type I IFN induction following chemotherapy treatment (related to Figure 4)

A. Cytosolic amount of gDNA and mtDNA in MC38 tumor cells treated with vehicle or the indicated chemotherapeutic drugs for 24 hr. Data are shown as mean±SEM (n=3). Two-way ANOVA and Sidak's multiple comparisons test were performed.

B. Real-time PCR analysis of *Ifnb* expression and cytosolic amount of mtDNA in MC38 tumor cells treated with vehicle or the indicated chemotherapeutic drugs for 24 hr, or plus with EtBr treatment for 4 days.

*, $P<0.05$; **, $P<0.01$; ***, $P<0.001$; ****, $P<0.0001$; ns, non significance

Figure S5. ROS-triggered oxidized mtDNA is critical for type I IFN induction by chemotherapy (related to Figure 5)

A. ATP production in the MC38 tumor cells after vehicle or the indicated chemotherapeutic drug treatment for 12 hr. Data are shown as mean±SEM (n=4). Two-way ANOVA and Sidak's multiple comparisons test were performed.

B. Flow analysis of ROS production in MC38 tumor cells after vehicle or PTX treatment for 24 hr. NT, no treatment; PC, positive control. Quantitative data are shown as mean±SEM (n=3). Two-tailed unpaired t-test was performed for the comparisons between two groups.

C. ELISA analysis of oxidized mtDNA marker 8-OHdG levels in MC38 tumor cells after vehicle or the indicated chemotherapeutic drug treatment for 24 hr. Data are shown as mean±SEM (n=3). Two-tailed unpaired t-test was performed for the comparisons between two groups.

D. Immunofluorescence staining of 8-OHdG in E0771 tumor cells after vehicle or PTX treatment for 24 hr. Scale bar, 50 μM.

E. ELISA analysis of oxidized mtDNA marker 8-OHdG levels in MC38 tumor cells after vehicle or the indicated chemotherapeutic drug treatment, or plus with antioxidants mito-TEMPO or NAC treatment for 24 hr. Data are shown as

mean±SEM (n=3). Two-tailed unpaired t-test was performed for the comparisons between two groups.

*, $P<0.05$; **, $P<0.01$; ***, $P<0.001$; ****, $P<0.0001$; ns, no significance

Figure S6. cGAS/STING-dependent oxidized mtDNA sensing drives type I IFN-mediated CD8$^+$ T cell anti-tumor immunity under chemotherapy (related to Figure 6)

A. Real-time PCR analysis of *Ifnb* expression in E0771 (left) of MC38 (right) tumor cells treated with vehicle or PTX for 24 hr, or plus with TLR9 inhibitor, RNA pol III inhibitor, STING inhibitor treatment for 24 hr. Data are shown as mean±SEM (n=3). Two-tailed unpaired t-test was performed for the comparisons between two groups.

B. Western blot validation of cGAS and STING deficiency of *Cgas*$^{-/-}$ and *Sting*$^{-/-}$ E0771 tumor cells established by CRISPR-Cas9.

C. Representative of flow analysis of Granzyme B staining in the tumor-infiltrating CD8$^+$ T cells of WT, *Cgas*$^{-/-}$, *Sting*$^{-/-}$ E0771-OVA-RFP tumor-bearing mice with vehicle or PTX treatment.

Figure S7. Antioxidant NAC impairs the therapeutic efficacy of chemotherapy and anti-PD-L1 blockade combination (related to Figure 7)

A. FACS analysis (above) and quantification (below) of levels of PD-L1 on the surface of MDA-MB-231 and BT549 breast cancer cells treated with vehicle or the indicated chemotherapeutic drugs PTX, DOX, CDDP for 24 hr or 48 hr. Quantitative data are shown as mean±SEM (n=3). Two-tailed unpaired t-test was

performed for the comparisons between two groups.

B. FACS analysis (left) and quantification (right) of PD-L1 expression on the surface of E0771 or 4T1 tumor cells treated with vehicle or STING agonist MSA-2, IFNβ treatment for 24 hr. Quantitative data are shown as mean±SEM (n=3). Two-tailed unpaired t-test was performed for the comparisons between two groups.

C. Analysis of TCGA database of the co-relation between cGAS, STING, type I IFN gene signatures and PD-L1 expression in colorectal cancer patients.

D. Analysis of TCGA database of the co-relation between type I IFN gene signatures and $CD8^+$T cell signatures in colorectal cancer patients.

*, $P<0.05$; **, $P<0.01$; ***, $P<0.001$; ****, $P<0.0001$

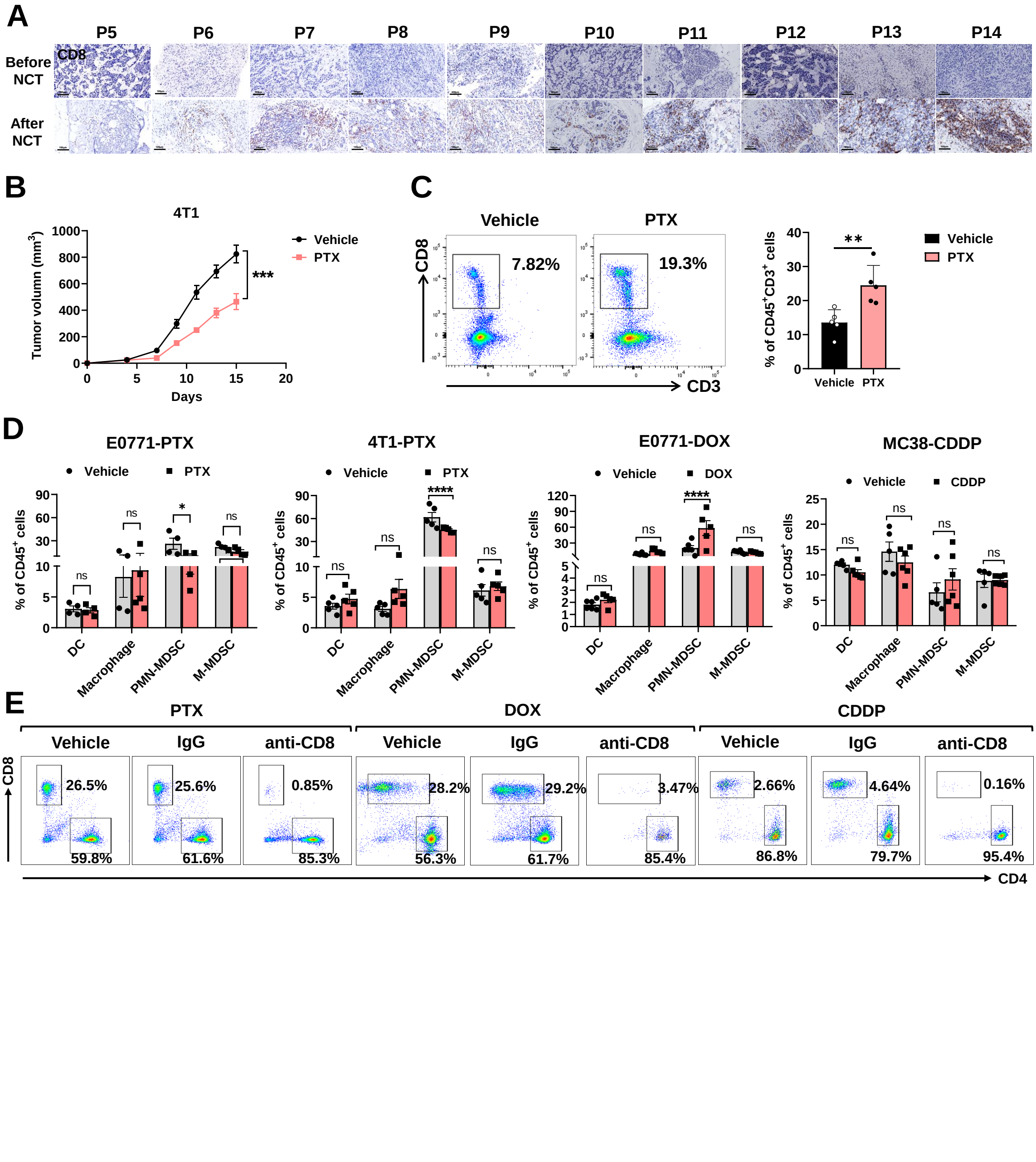
A
P5
P6
P7
P8
P9
P10
P11
P12
P13
P14
Before NCT
After NCT
CD8
B
4T1
Tumor volumn (mm3)
Days
Vehicle
PTX
***
C
Vehicle
PTX
CD8
CD3
7.82%
19.3%
% of CD45+CD3+ cells
**
D
E0771-PTX
4T1-PTX
E0771-DOX
MC38-CDDP
% of CD45+ cells
DOX
CDDP
DC
Macrophage
PMN-MDSC
M-MDSC
ns
E
PTX
DOX
CDDP
IgG
anti-CD8
26.5%
59.8%
25.6%
61.6%
0.85%
85.3%
28.2%
56.3%
29.2%
61.7%
3.47%
85.4%
2.66%
86.8%
4.64%
79.7%
0.16%
95.4%
CD4

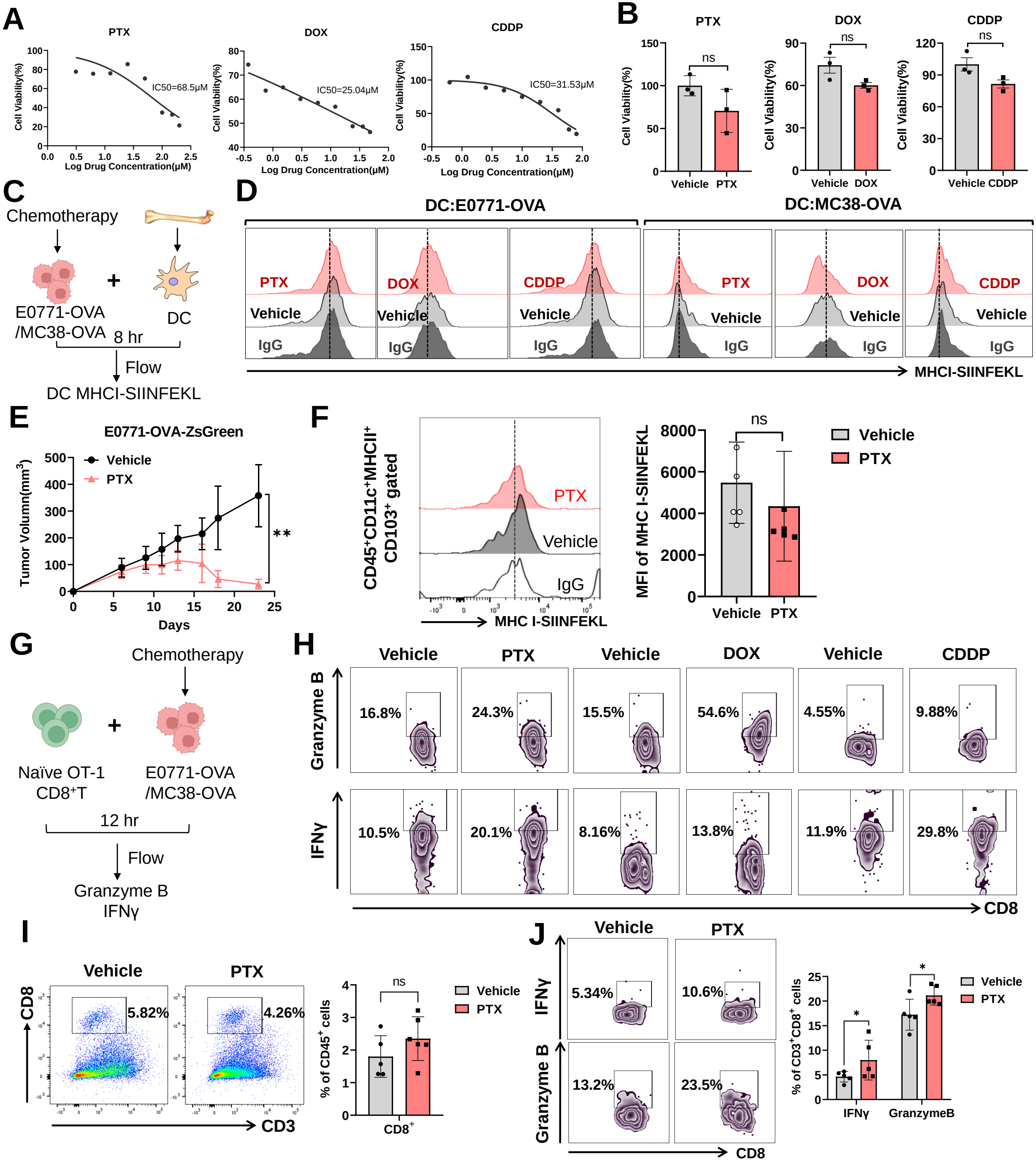
A
PTX
DOX
CDDP
Cell Viability(%)
IC50=68.5μM
IC50=25.04μM
IC50=31.53μM
Log Drug Concentration(μM)
B
PTX
DOX
CDDP
ns
Cell Viability(%)
Vehicle
PTX
DOX
CDDP
C
Chemotherapy
E0771-OVA
/MC38-OVA
DC
8 hr
Flow
DC MHCI-SIINFEKL
D
DC:E0771-OVA
DC:MC38-OVA
PTX
DOX
CDDP
Vehicle
IgG
MHCI-SIINFEKL
E
E0771-OVA-ZsGreen
Vehicle
PTX
Tumor Volumn(mm3)
**
Days
F
CD45+CD11c+MHCII+
CD103+ gated
PTX
Vehicle
IgG
MHC I-SIINFEKL
MFI of MHC I-SIINFEKL
ns
Vehicle
PTX
G
Chemotherapy
Naïve OT-1
CD8+T
E0771-OVA
/MC38-OVA
12 hr
Flow
Granzyme B
IFNγ
H
Vehicle
PTX
DOX
CDDP
Granzyme B
IFNγ
16.8%
24.3%
15.5%
54.6%
4.55%
9.88%
10.5%
20.1%
8.16%
13.8%
11.9%
29.8%
CD8
I
Vehicle
PTX
CD8
CD3
5.82%
4.26%
% of CD45+ cells
CD8+
ns
Vehicle
PTX
J
Vehicle
PTX
IFNγ
Granzyme B
5.34%
10.6%
13.2%
23.5%
CD8
% of CD3+CD8+ cells
IFNγ
GranzymeB
*
*
Vehicle
PTX

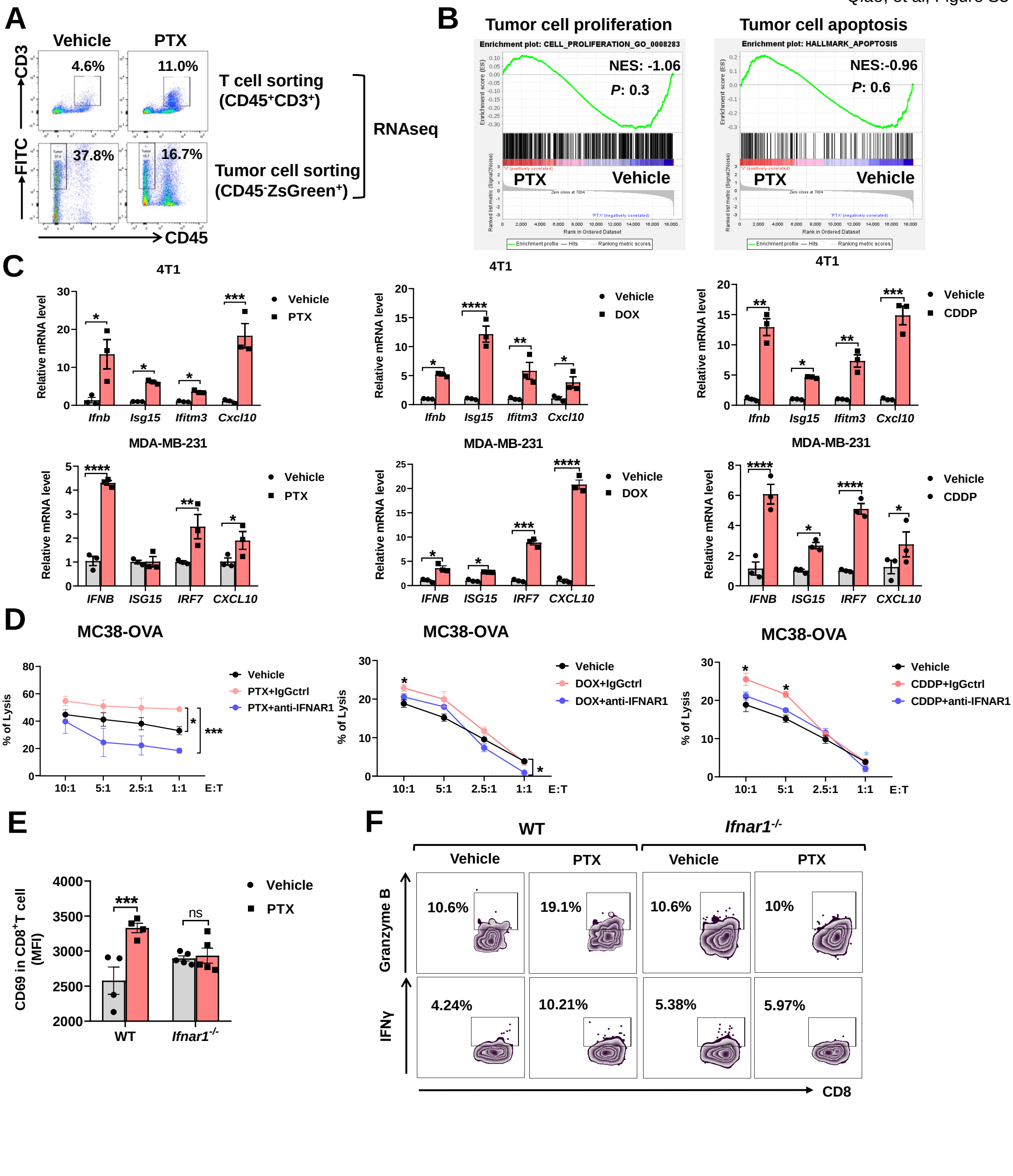
A
Vehicle
PTX
CD3
FITC
CD45
4.6%
11.0%
37.8%
16.7%
T cell sorting
(CD45+CD3+)
Tumor cell sorting
(CD45-ZsGreen+)
RNAseq
B
Tumor cell proliferation
Tumor cell apoptosis
Enrichment plot: CELL_PROLIFERATION_GO_0008283
Enrichment plot: HALLMARK_APOPTOSIS
NES: -1.06
P: 0.3
NES:-0.96
P: 0.6
PTX
Vehicle
Enrichment score (ES)
Ranked list metric (Signal2Noise)
Rank in Ordered Dataset
Enrichment profile
Hits
Ranking metric scores
C
4T1
MDA-MB-231
Relative mRNA level
Vehicle
PTX
DOX
CDDP
Ifnb
Isg15
Ifitm3
Cxcl10
IFNB
ISG15
IRF7
CXCL10
D
MC38-OVA
% of Lysis
PTX+IgGctrl
PTX+anti-IFNAR1
DOX+IgGctrl
DOX+anti-IFNAR1
CDDP+IgGctrl
CDDP+anti-IFNAR1
10:1
5:1
2.5:1
1:1
E:T
E
CD69 in CD8+T cell (MFI)
WT
Ifnar1-/-
ns
F
Granzyme B
IFNγ
CD8
10.6%
19.1%
10.6%
10%
4.24%
10.21%
5.38%
5.97%

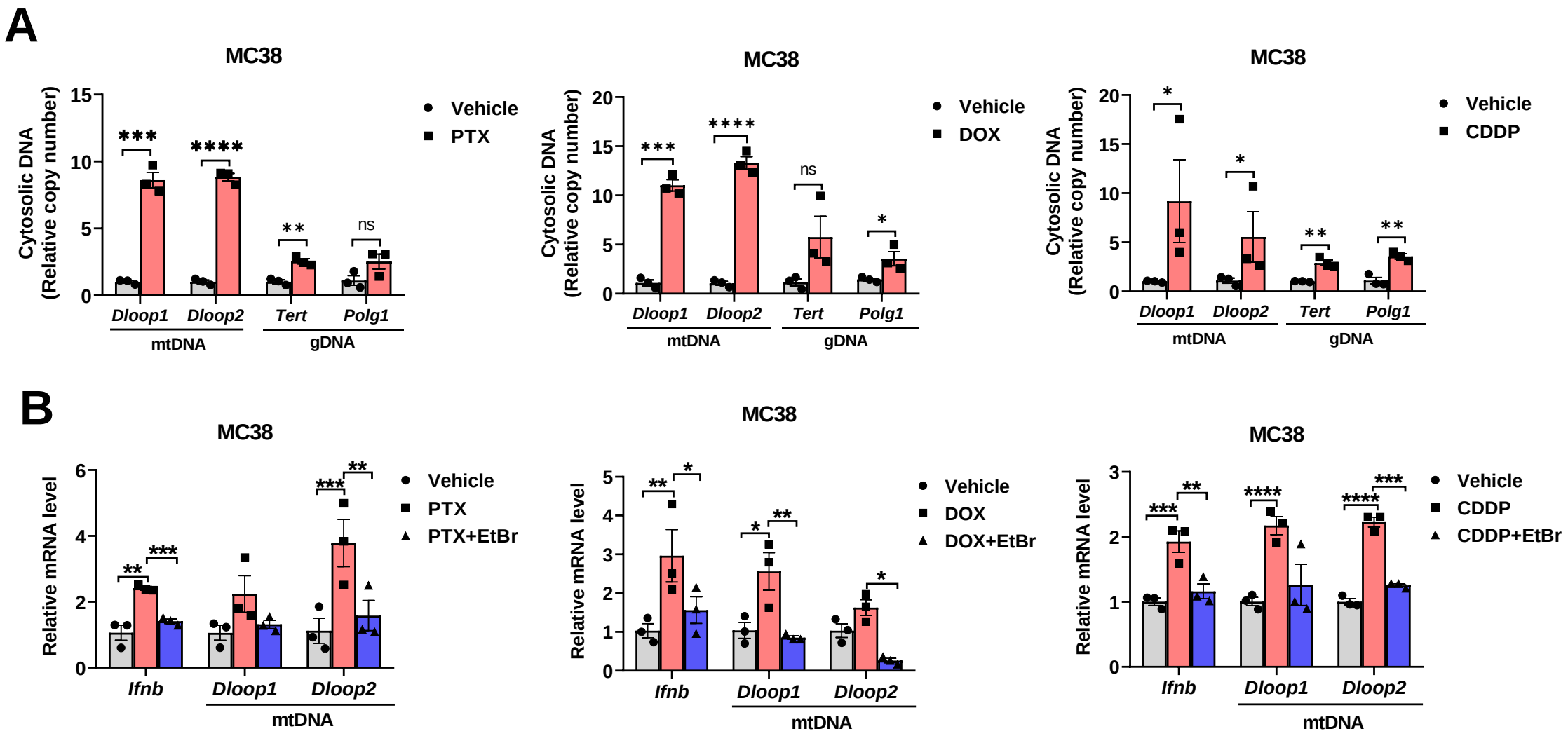
A
MC38
Cytosolic DNA (Relative copy number)
Vehicle
PTX
DOX
CDDP
Dloop1
Dloop2
Tert
Polg1
mtDNA
gDNA
ns
B
Relative mRNA level
PTX+EtBr
DOX+EtBr
CDDP+EtBr
Ifnb

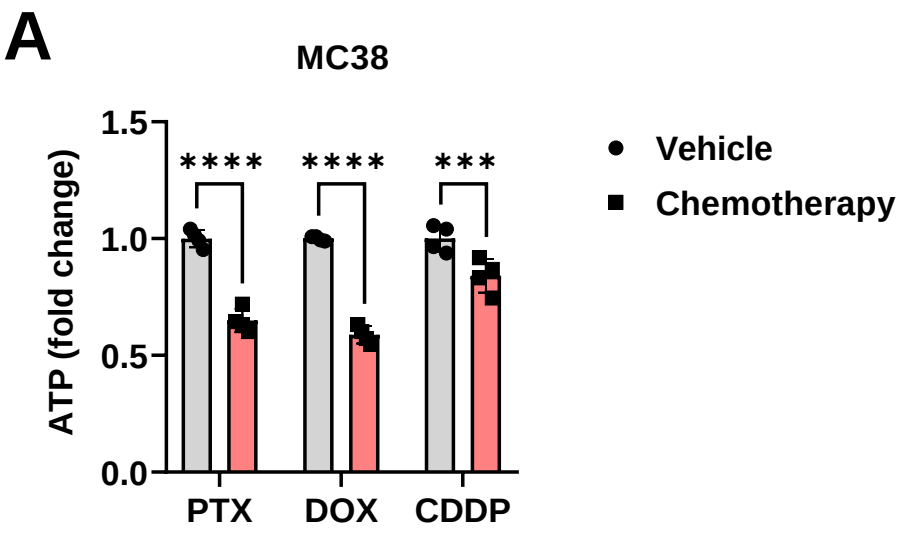
A
MC38
ATP (fold change)
1.5
1.0
0.5
0.0
****
****
***
PTX
DOX
CDDP
Vehicle
Chemotherapy

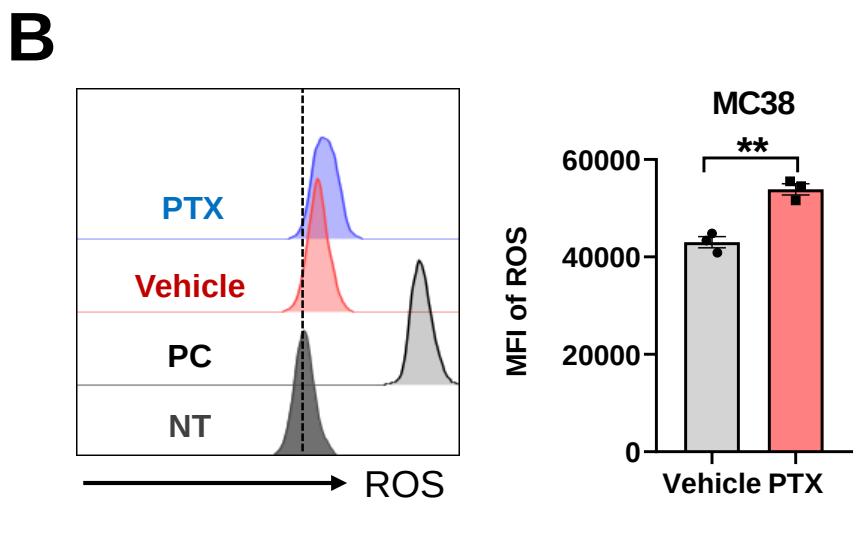
B
PTX
Vehicle
PC
NT
ROS
MC38
MFI of ROS
60000
40000
20000
0
**
Vehicle
PTX

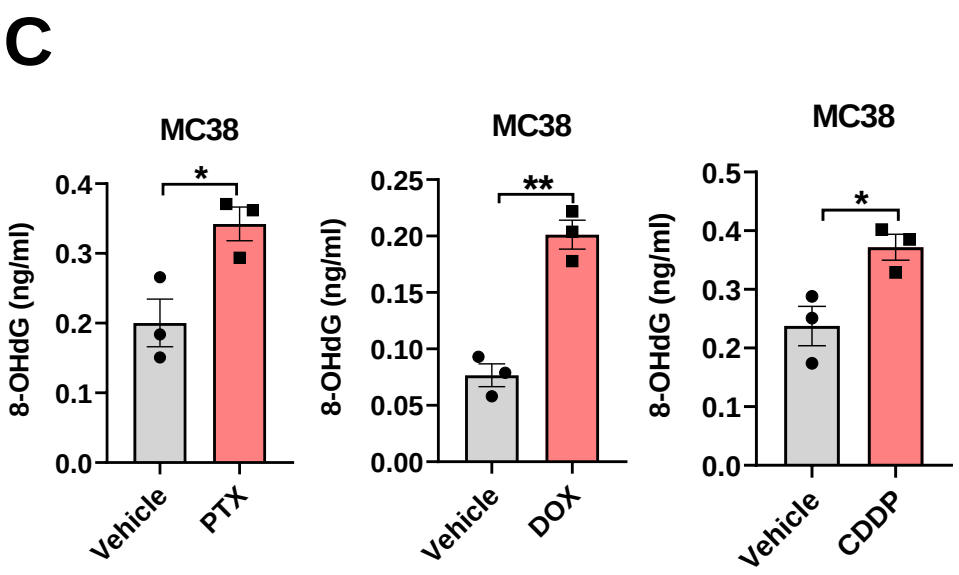
C
MC38
8-OHdG (ng/ml)
0.4
0.3
0.2
0.1
0.0
*
Vehicle
PTX
MC38
8-OHdG (ng/ml)
0.25
0.20
0.15
0.10
0.05
0.00
**
Vehicle
DOX
MC38
8-OHdG (ng/ml)
0.5
0.4
0.3
0.2
0.1
0.0
*
Vehicle
CDDP

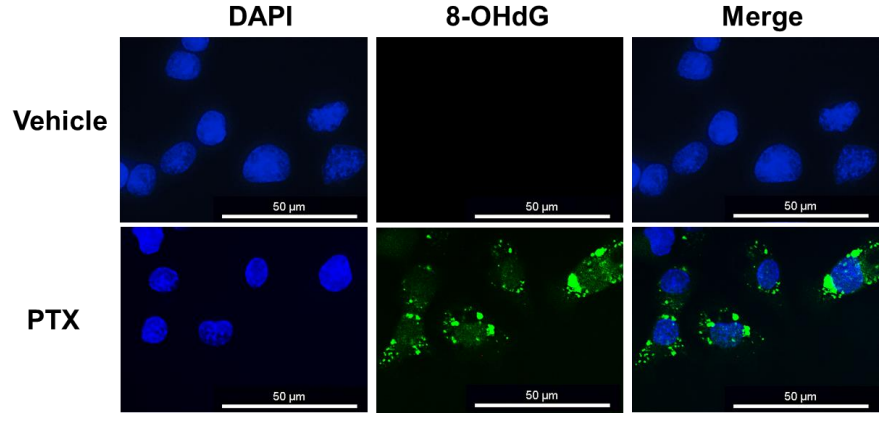
D
DAPI
8-OHdG
Merge
Vehicle
PTX
50 μm

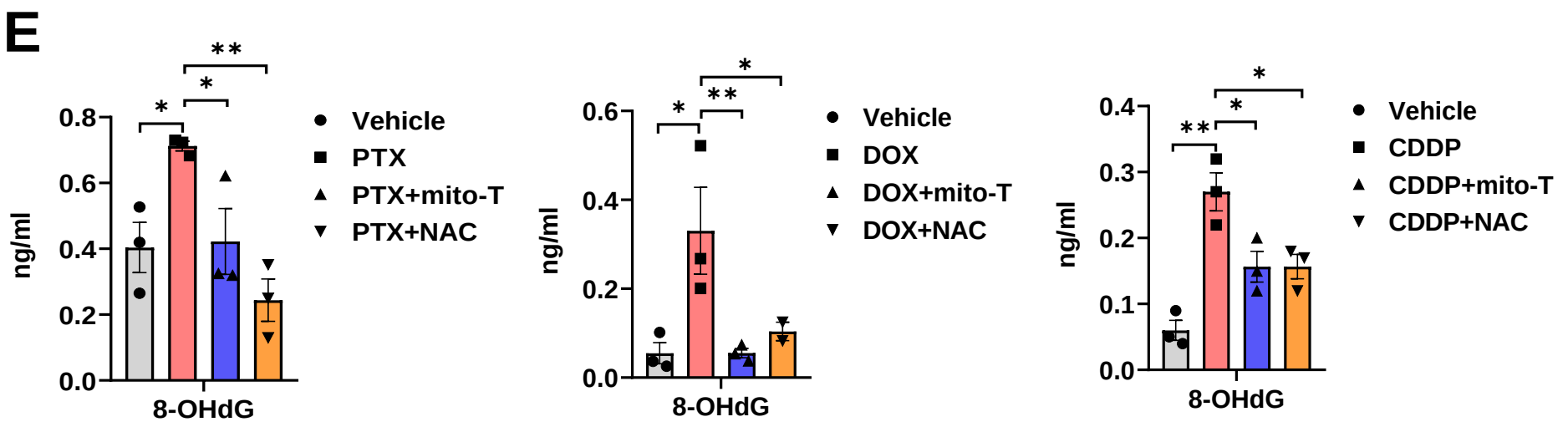
E
ng/ml
0.8
0.6
0.4
0.2
0.0
*
*
8-OHdG
Vehicle
PTX
PTX+mito-T
PTX+NAC
ng/ml
0.6
0.4
0.2
0.0
*
**
*
8-OHdG
Vehicle
DOX
DOX+mito-T
DOX+NAC
ng/ml
0.4
0.3
0.2
0.1
0.0
**
*
*
8-OHdG
Vehicle
CDDP
CDDP+mito-T
CDDP+NAC

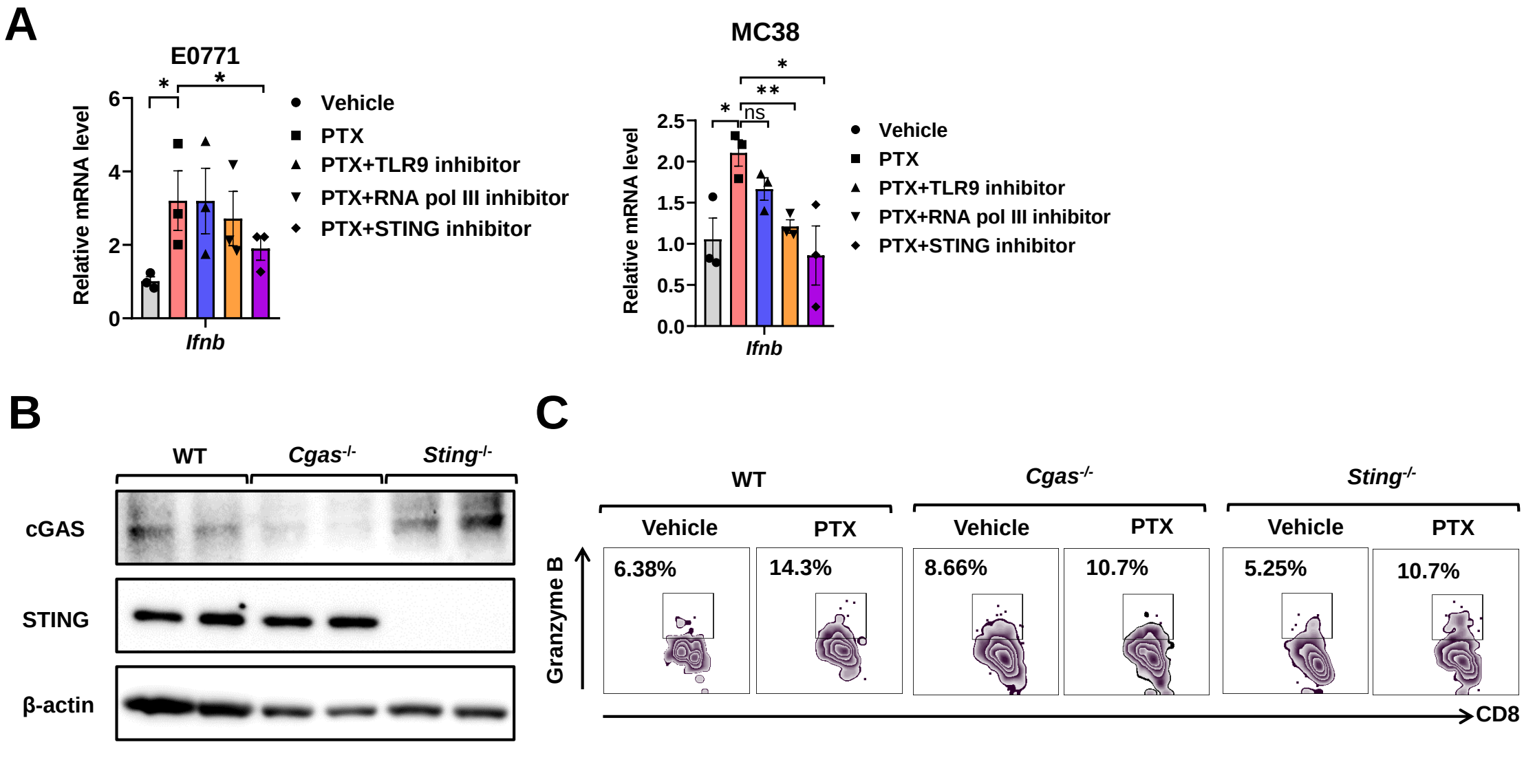
A
E0771
Relative mRNA level
6
4
2
0
*
*
Ifnb
Vehicle
PTX
PTX+TLR9 inhibitor
PTX+RNA pol III inhibitor
PTX+STING inhibitor
MC38
Relative mRNA level
2.5
2.0
1.5
1.0
0.5
0.0
*
**
*
ns
Ifnb
Vehicle
PTX
PTX+TLR9 inhibitor
PTX+RNA pol III inhibitor
PTX+STING inhibitor
B
WT
Cgas-/-
Sting-/-
cGAS
STING
β-actin
C
WT
Cgas-/-
Sting-/-
Vehicle
PTX
Vehicle
PTX
Vehicle
PTX
Granzyme B
6.38%
14.3%
8.66%
10.7%
5.25%
10.7%
CD8

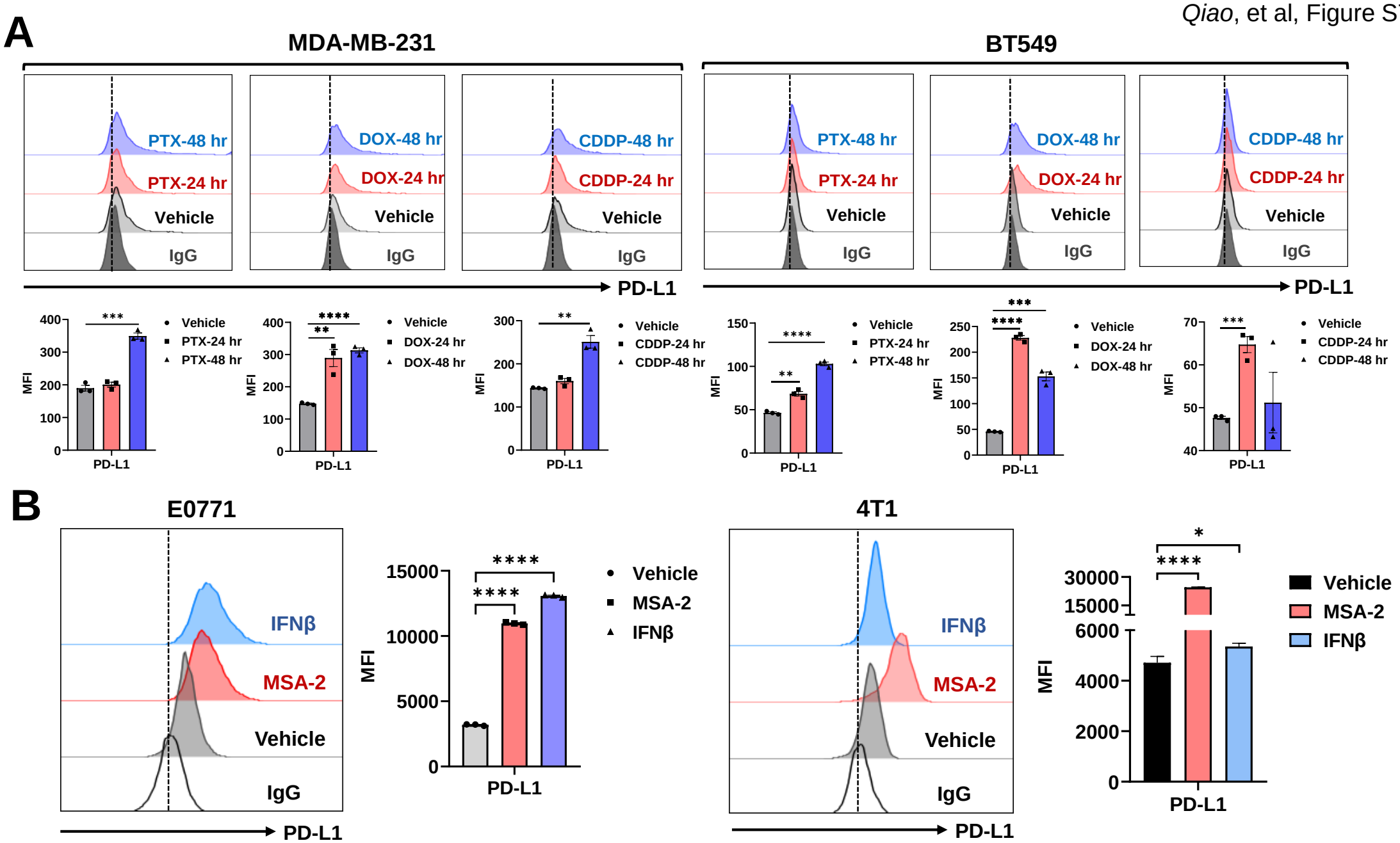
A
MDA-MB-231
BT549
PTX-48 hr
PTX-24 hr
DOX-48 hr
DOX-24 hr
CDDP-48 hr
CDDP-24 hr
Vehicle
IgG
PD-L1
MFI
Vehicle
PTX-24 hr
PTX-48 hr
DOX-24 hr
DOX-48 hr
CDDP-24 hr
CDDP-48 hr
B
E0771
4T1
IFNβ
MSA-2
Vehicle
IgG
PD-L1
MFI
C
COAD
cGAS vs PD-L1
p−value = 2.5e−12
R = 0.41
Log2(PDL1)
Log2(cGAS)
COAD
STING vs PD-L1
p−value = 0.007
R = 0.16
Log2(PDL1)
Log2(STING)
COAD
IFN-I vs PD-L1
p−value = 0
R = 0.53
Log2(PD-L1)
Log2(Type I IFN Signature)
D
COAD
IFN-I vs CD8+ T
p−value = 0
R = 0.7
Log2(CD8 T cell Signature)
Log2(Type I IFN Signature)